CHEST

Use of CT Imaging to Quantify Progression and Response to Treatment in Lymphangioleiomyomatosis

Vissaagan Gopalakrishnan, BS; Jianhua Yao, PhD; Wendy K. Steagall, PhD; Nilo A. Avila, MD; Angelo M. Taveira-DaSilva, MD, PhD; Mario Stylianou, PhD; Marcus Y. Chen, MD; and Joel Moss, MD, PhD

BACKGROUND: In lymphangioleiomyomatosis (LAM), infiltration of the lungs with smooth muscle-like LAM cells results in cystic destruction and decline in lung function, effects stabilized by sirolimus therapy. LAM lung disease is followed, in part, by high-resolution CT scans. To obtain further information from these scans, we quantified changes in lung parenchyma by analyzing image "texture."

METHODS: Twenty-six texture properties were quantified by analyzing the distribution and intensity of pixels with a computer-aided system. Both cross-sectional and longitudinal studies were performed to examine the relationships between texture properties, cyst score (percentage of lung occupied by cysts), FEV_1, and diffusion capacity for carbon monoxide (D_{LCO}), and to determine the effect of sirolimus treatment.

RESULTS: In the cross-sectional study, 18 texture properties showed significant positive correlations with cyst score. Cyst score and 13 of the 18 texture properties showed significant differences in rates of change after sirolimus treatment; 11 also significantly predicted FEV_1 and D_{LCO}.

CONCLUSIONS: Increased cyst score was associated with increased texture degradation near cysts. Sirolimus treatment improved lung texture surrounding cysts and stabilized cyst score. Eleven texture properties were associated with FEV_1, D_{LCO}, cyst score, and response to sirolimus. Texture analysis may be valuable in evaluating LAM severity and treatment response.

CHEST 2019; 155(5):962-971

KEY WORDS: CT imaging; function; lymphangioleiomyomatosis; pulmonary; sirolimus

ABBREVIATIONS: D_{LCO} = diffusion capacity for carbon monoxide; HRCT = high-resolution CT; LAM = lymphangioleiomyomatosis; TSC = tuberous sclerosis complex

AFFILIATIONS: From the Pulmonary Branch (Drs Steagall, Avila, Taveira-DaSilva, and Moss; and Mr Gopalakrishnan), National Heart, Lung, and Blood Institute, National Institutes of Health, Bethesda, MD; Rush Medical College (Dr Gopalakrishnan), Rush University Medical Center, Chicago, IL; Radiology and Imaging Sciences Department (Dr Yao), National Institutes of Health, Bethesda, MD; Radiology Service (Dr Avila), Washington DC Veterans Affairs Medical Center, Washington, DC; Office of Biostatistics Research (Dr Stylianou), National Heart, Lung, and Blood Institute, National Institutes of Health, Bethesda, Maryland; and Cardiovascular Branch (Dr Chen), National Heart, Lung, and Blood Institute, National Institutes of Health, Bethesda, MD.

FUNDING/SUPPORT: This study was funded by the Intramural Research Program, National Institutes of Health (NIH), National Heart, Lung, and Blood Institute, and the NIH Medical Research Scholars Program, a public-private partnership supported jointly by the NIH and generous contributions to the Foundation for the NIH from the Doris Duke Charitable Foundation, the American Association for Dental Research, the Colgate-Palmolive Company, Genentech, and other private donors. For a complete list, visit the Foundation website at http://www.fnih.org.

CORRESPONDENCE TO: Joel Moss, MD, PhD, Pulmonary Branch, National Heart, Lung, and Blood Institute, National Institutes of Health, Room 6D05, Bldg 10, 9000 Rockville Pike, Bethesda, MD 20892; e-mail: mossj@nhlbi.nih.gov

DOI: https://doi.org/10.1016/j.chest.2019.01.004

Lymphangioleiomyomatosis (LAM), a multisystem disease that primarily affects premenopausal women, is characterized by cystic lung destruction, lymphatic involvement (eg, chylous effusions), and abdominal tumors (eg, angiomyolipomas).[1-4] LAM occurs sporadically or in association with tuberous sclerosis complex (TSC), an inherited neurocutaneous disorder.[5,6] Neoplastic LAM cells have smooth muscle characteristics and harbor inactivating *TSC1* or *TSC2* mutations.[5-7] The loss of function of proteins encoded by the TSC genes results in constitutive activation of mechanistic target of rapamycin signaling, which is responsible for cell growth, size, and survival.[8]

The Multicenter International Lymphangioleiomyomatosis Efficacy and Safety (MILES) trial showed that sirolimus therapy stabilized lung function and was associated with reduction in symptoms and improved quality of life.[9] Further studies showed that sirolimus slows changes in lung volume occupied by cysts[10] and decreases the size of renal angiomyolipomas[11,12] and chylous effusions.[13]

Monitoring of disease progression in LAM is accomplished by serial measurement of lung function[4]; however, this testing requires patient cooperation and exertion, and may fail to uncover gas exchange abnormalities that manifest only during exercise testing. High-resolution CT (HRCT) scans of the chest are used in the diagnosis and evaluation of LAM.[1,4] The regular collection of HRCT scans makes LAM an appropriate model for the development of image processing techniques to quantify disease progression and treatment response. Although radiation exposure is a risk of serial CT studies, advances in low-dose chest CT imaging have led to improvement in image quality,[14,15] and low-dose imaging has been used in screening for lung cancer.[16,17]

Radiologic studies have analyzed the lung and established correlations to physiologic data. In LAM, these include calculations of a disease-specific radiologic score, determinations of areas with lower attenuation, or the percent of lung volume occupied by cysts (cyst score).[18-21] Beyond cyst score calculation, other image processing techniques can be applied, such as pixel-level analysis of CT images. The distribution of pixels of various intensity yields an "image texture" that can be quantified by distinct mathematical calculations that highlight different attributes of texture.[22-24] This image texture can be used quantitatively to detect emphysema, pulmonary nodules, pulmonary embolism, and other abnormalities,[25] and to classify pulmonary tissue patterns into different categories (eg, nodular, ground-glass, emphysematous).[26,27]

In LAM, we identified emphysematous-like changes in lung areas adjacent to cysts both radiologically and histologically,[20] and found that some texture properties correlated with FEV_1 and lung diffusion capacity for carbon monoxide (D_{LCO}).[20] These texture properties allowed identification and quantification of areas in the vicinity of LAM cysts, were associated with disease severity, and permitted assessment of lung tissue around the cysts. Overall, these textural imaging changes were associated with changes in tissue degradation.[20] A study of 12 patients with LAM showed that presirolimus rates of change in the lung parenchyma as measured by texture properties tended to be greater than, but not significantly different ($P = .13$) from, changes in texture during treatment.[10]

The aim of this study was to compare and validate methods of calculating texture in tracking LAM disease progression and treatment as defined by FEV_1, D_{LCO}, and cyst score. A cross-sectional study examined the association of cyst score with texture properties. Texture properties showing significant findings were then analyzed in the longitudinal study, assessing the effect of sirolimus treatment on the rate of texture changes.

Materials and Methods

Complete descriptions of all methods are in e-Appendix 1.

Patient Population

This study was approved by the National Heart, Lung, and Blood Institute Institutional Review Board (Protocols 95-H-0186 and 96-H-0100). All patients provided written informed consent. Patients received a diagnosis of LAM on the basis of American Thoracic Society and/or European Respiratory Society guidelines.[1,4]

One hundred thirty-five women with LAM (age 49 ± 10 years) participated in a cross-sectional study (Table 1). Thirty-five women with LAM who were treated with sirolimus (age 45 ± 10.6 years at the start of treatment) were studied in a longitudinal study (Table 1). There was no overlap between the two study populations.

Pulmonary Function Testing

FEV_1 and D_{LCO} were measured during the same hospital visit with a CT examination per American Thoracic Society/European Respiratory Society standards.[28,29]

Radiologic Methods, Lung Segmentation, and Cyst Detection

HRCT scans of the chest were performed with the patients in a prone position because this position minimizes the compression of the lungs by the heart. The radiation dose for obtaining select images of the lungs

TABLE 1] Demographics and Clinical Data of 35 Patients With LAM Studied Longitudinally and 135 Patients With LAM Studied at a Single Time Point per Patient

Category	Longitudinal Study	Cross-Sectional Study
No. of patients	35	135
Demographics		
Caucasian	31 (89)	108 (80)
African American	0	9 (7)
Asian	2 (6)	8 (6)
Hispanic	2 (6)	5 (4)
Other	0	5 (4)
Clinical characteristics		
Age of diagnosis, y	34 ± 10.8	41 ± 9.9
Age of initial symptoms, y	35 ± 9.4	38 ± 11.0
TSC	6 (17)	20 (15)
Oxygen therapy	22 (63)	32 (24)
Lymphangioleiomyomas	19 (54)	37 (27)
Angiomyolipomas	18 (51)	62 (46)

Data are presented as No. (%) unless otherwise indicated. LAM = lymphangioleiomyomatosis; TSC = tuberous sclerosis complex.

is over 6 fold lower than a standard chest CT with coverage of the chest.[30] Cystic regions and total lung areas were calculated for every slice in a CT examination, yielding a total percent of lung volume occupied by cysts (cyst score) (Fig 1).

Texture Analysis

Texture properties are established mathematical calculations used to quantify the distribution and intensity of pixels in a selected region of an image.[22-24] Twenty-six texture properties, falling under three categories (histogram measures, co-occurrence matrix measures, and run-length measures), were calculated for each HRCT (Table 2). Histogram measures describe the spread of values and do not incorporate spatial information. Co-occurrence matrix measures calculate how often pairs of pixels with specific intensities occur adjacent to each other, whereas run-length measures describe the continuity of signal by identifying "runs," which are strings of pixels with the same intensity in a certain orientation.

Data Analysis and Statistical Methods

Cross-sectional Study: Linear regression of cyst score vs 26 texture properties was computed. Texture properties with significant ($P < .05$) correlations with cyst score were identified and analyzed further in the longitudinal study.

Longitudinal Study: Multiple HRCTs and pulmonary function measurements for each patient were plotted over time. Mixed effects models were used to incorporate within-subject and between-subject variability, as well as repeated measures. Yearly rates of change in cyst score, texture properties, FEV_1, and D_{LCO} were calculated using mixed effects models, adjusting for initial values and sirolimus

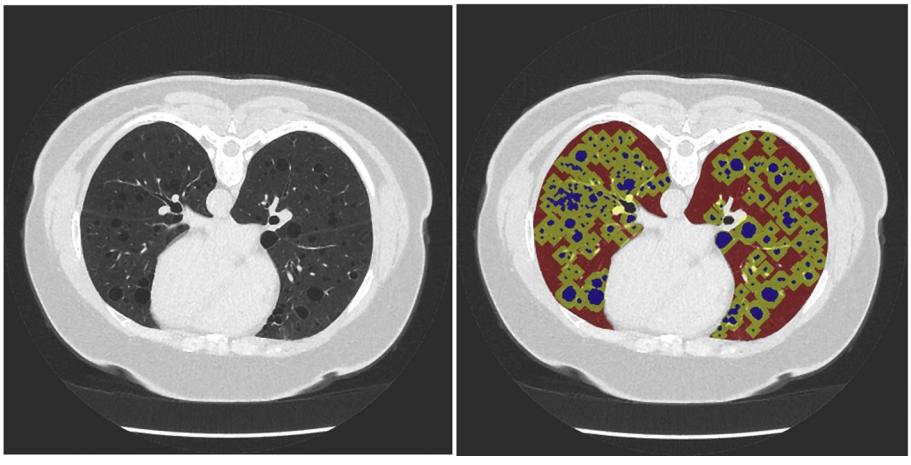

Figure 1 – *Selection of cystic regions (blue), regions near cysts (yellow), and regions away from cysts (red) in a CT examination of a patient with lymphangioleiomyomatosis. For every slice in a CT study, areas occupied by cysts are summed and divided by total lung area, yielding the cyst score (the percentage of lung occupied by cysts). Image texture is calculated in all regions <10 mm from cysts (yellow) and all regions >10 mm away from cysts (red) and averaged across all slices. The difference in texture between regions near and away was used as a measure of lung parenchymal degradation. Increases in texture measures suggest increased degradation of lung parenchyma surrounding cysts.*

TABLE 2] Categories of Texture Properties Calculated on Chest HRCT Scans

Texture Category	Description	Texture Name
Histogram measures	Describe spread of values in a figure that plots frequency of pixels with a certain intensity	Mean
		Variance
		Skewness
		Kurtosis
		Absolute deviation
		SD
Co-occurrence matrix measures	Calculate how often pairs of pixels with specific intensities occur adjacent to each other	Energy
		Inertia
		Inverse difference
		Entropy
		Correlation
		Sum entropy
		Difference entropy
		Sum average
		Difference average
Run-length measures	Describe continuity of signal by identifying "runs," which are strings of pixels with the same intensity in a certain orientation	Short run emphasis
		Long run emphasis
		Gray-level nonuniformity
		Run-length nonuniformity
		Run percentage
		Low gray-level run emphasis
		High gray-level run emphasis
		Short run low-gray emphasis
		Short run high-gray emphasis
		Long run low-gray emphasis
		Long run high-gray emphasis

HRCT = high-resolution CT.

treatment. Unadjusted, other than the initial value of each outcome, associations of pulmonary function (FEV_1 and DLCO) and cyst score against texture properties were also obtained.

Establishment of Method of Analysis of Texture Properties

We have previously calculated cyst scores and texture properties for patients with LAM and compared them with pulmonary function tests.[10,20] Some texture properties and cyst scores were significantly associated with FEV_1 and DLCO. We did not show a significant effect of sirolimus on the rate of change cyst scores or texture properties before vs during treatment, although a trend was noted for improvement in lung parenchyma during treatment.[10] This may be due to the small sample size (12 patients) and the difficulty in comparing texture properties calculated on HRCT scans performed on different CT scanners over time. In this study, we have expanded the population studied longitudinally to 35 patients (including 11 of the 12 previously studied[10]). We also used the difference in texture properties near and away from cysts, so that we had texture measurements that have an internal control for the HRCT scan itself and thus can be compared across CT scans from different machines.

To show that texture values away from cysts can be used as stable controls for the texture values near cysts, we examined the texture properties near and away from cysts over time. After the cysts are identified by the computer, all regions near cysts (< 10 mm) and away from cysts (> 10 mm) were selected (Fig 1). For example, the values of the texture property energy at least 10 mm away from cysts 5 years before sirolimus treatment were not significantly different from textures at the start of treatment despite decline in lung function and increase in cyst score; however, energy values near cysts varied significantly ($P = .004$) (Fig 2). All 26 texture properties were examined, and stable areas far from the cysts were found for each; therefore, texture values at least 10 mm away from cysts served as suitable controls to measure texture changes near cysts. The difference in texture (absolute value) between regions near and away from cysts was used to measure the degradation of lung texture.

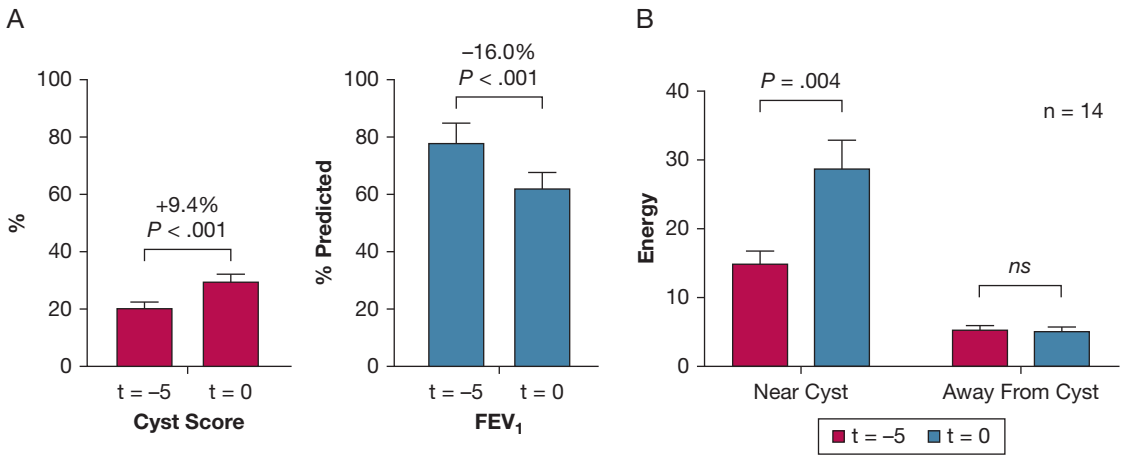

Figure 2 – *The difference in texture (absolute value) between regions near and away from cysts can be used to measure the degradation of lung parenchyma and to control for technical differences resulting from type of CT scanner used. A, Comparison of cyst score and FEV_1 at 5 years before starting sirolimus treatment (t = –5) and at the start of sirolimus treatment (t = 0) in 14 patients using a paired t test. B, Comparison of energy near cysts (< 10 mm) and away from cysts (> 10 mm) at t = –5 and t = 0 in 14 patients using a paired t test. Energy is a texture property (co-occurrence matrix measure) with significant (P < .001) correlations to FEV_1, diffusion capacity for carbon monoxide, and cyst score (R = 0.79). Energy is used here for illustrative purposes; all 26 texture properties were examined, and stable areas far from cysts were found for each. NS = not significant.*

Results

Correlation of Cyst Score and Lung Texture

Linear regressions and correlations of 26 texture properties vs cyst score were computed (Table 3). Eighteen texture properties showed statistically significant correlations with cyst score. Almost all significant correlations had a positive slope, indicating that the texture difference between regions near cysts and away from cysts increased as cyst score increased.

Comparison of Lung Texture, Pulmonary Function, and Cyst Score Change Rates Before and During Sirolimus Treatment

Mixed effects models were used to compare the rates of change in FEV_1, DLCO, cyst score, and texture properties before and during sirolimus treatment (Table 4). Analysis was conducted on texture properties that showed significant correlations with cyst score. Before sirolimus treatment, annual rates of decline in FEV_1 and DLCO were 2.61 ± 0.24% and 2.20 ± 0.21% predicted, respectively. During treatment, annual rates of decline in FEV_1 and DLCO were 0.32 ± 0.34% and 0.48 ± 0.30% predicted, respectively (both $P < .001$). Before sirolimus treatment, cyst scores increased at an annual rate of 0.93 ± 0.15%. During treatment, cyst scores decreased at an annual rate of 0.14 ± 0.22% ($P < .001$).

Before treatment, the difference in texture between regions near cysts and away from cysts increased in all but one of the 18 texture properties. After treatment, the annual rates of change in all texture properties were negative, indicating a decrease in the texture difference between regions near and away from cysts. Thirteen texture properties showed significant changes in rate (all $P < .005$) (Table 4). Of the 13 properties, 11 were also significantly associated with FEV_1, DLCO, and cyst score (all $P \leq .017$) in visits before sirolimus treatment and in all visits (Table 5). The texture properties "kurtosis" and "mean" showed statistically significant changes in rate during sirolimus treatment ($P = .009$ and $< .001$, respectively), but did not correlate significantly with FEV_1 or DLCO in visits before sirolimus treatment and in all visits (Table 5).

Discussion

Our study shows that certain texture properties generated from HRCT scans reflect changes in lung parenchyma in areas surrounding cysts in LAM. In a cross-sectional study of patients, we determined the effect of increasing cyst score on texture changes in lung parenchyma surrounding cysts. The texture properties that were significant in the cross-sectional study were then examined in a longitudinal study looking at differences in the rate of change of texture before and during sirolimus treatment. Among the 13 texture properties that had significantly different rates of change after initiation of sirolimus treatment, 11 were also found to correlate significantly with FEV_1 and DLCO. These data indicate that texture properties have the potential to serve as markers of LAM disease status and progression.

The cross-sectional and longitudinal studies provide a new understanding of LAM lung disease progression and

TABLE 3] Linear Regression Results for 26 Texture Properties Compared With Cyst Score (% of Lung Occupied by Cysts) in 135 Chest HRCTs of Patients With LAM

Texture Property	Texture Category	*P*	R
Mean	**Histogram**	**< .001**	**0.524**
Variance	Histogram	.208	−0.108
Skewness	**Histogram**	**.0051**	**0.238**
Kurtosis	**Histogram**	**.0042**	**0.243**
Absolute deviation	Histogram	.661	−0.038
SD	Histogram	.571	−0.049
Energy	**CM**	**< .001**	**0.799**
Inertia	CM	.546	−0.052
Inverse difference	CM	**< .001**	**0.729**
Entropy	**CM**	**< .001**	**0.756**
Correlation	CM	.724	−0.030
Sum entropy	CM	**< .001**	**0.745**
Difference entropy	CM	**< .001**	**0.733**
Sum average	**CM**	**.029**	**0.187**
Difference average	**CM**	**< .001**	**0.286**
Short run emphasis	**RL**	**< .001**	**0.752**
Long run emphasis	**RL**	**< .001**	**0.800**
Gray-level nonuniformity	**RL**	**< .001**	**0.493**
Run-length nonuniformity	**RL**	**< .001**	**0.737**
Run percentage	**RL**	**< .001**	**0.788**
Low-gray run emphasis	**RL**	**< .001**	**0.737**
High-gray emphasis	RL	.953	0.005
Short run low-gray emphasis	RL	**.007**	**-0.229**
Short run high-gray emphasis	RL	.758	0.027
Long run low-gray emphasis	**RL**	**< .001**	**0.841**
Long run high-gray emphasis	RL	.522	−0.055

All textures values were plotted as the difference in texture near cysts compared with away from cysts. Texture properties in bold showed statistically significant correlation with cyst score after adjustment for initial cyst score. CM = co-occurrence matrix; RL = run-length.

response to sirolimus treatment. Because the percent of lung occupied by cysts increases, texture changes around cysts are consistent with parenchymal degradation. This was demonstrated by positive correlations between cyst score and the difference in texture between regions near cysts and away from cysts (Table 3). From the longitudinal study, we found that sirolimus reverses decline in texture surrounding cysts (Table 4). The magnitude of the rate of texture improvement during sirolimus treatment is generally much lower than the rate of texture decline before treatment. Cyst scores also show slow improvement during treatment. These findings suggest that sirolimus may have a profound effect on lung parenchyma and cyst formation.

Although cyst formation in LAM is poorly understood, it is likely driven by LAM cell-mediated overexpression of matrix metalloproteinases and decreased expression of the tissue inhibitor of metalloproteinase-1, leading to aberrant destruction of lung epithelium and connective tissue.[31] Inhibition of mechanistic target of rapamycin, a coordinator of cell growth and proliferation,[8] by sirolimus may decrease LAM cell activity, resulting in decreased protease-driven lung damage and greater opportunity for lung repair. Furthermore, sirolimus has also been shown to increase expression of connective tissue growth factor (CCN2) and migration of lung fibroblasts,[32] which could explain the reversal of lung parenchymal destruction during sirolimus treatment.

We have identified 11 texture properties that track lung changes in LAM, all of which incorporate spatial information into their calculations (Table 2), suggesting that the use of spatial information in calculating texture

TABLE 4] Comparison of Mean Rates of Change per Year Before and After Sirolimus Treatment for PFTs (FEV_1, D_{LCO}), Cyst Score, and 18 Texture Properties of 35 Patients Using Mixed Effects Models

	Parameter	Mean Pretreatment Rate	Mean Posttreatment Rate	*P* Value
	FEV_1, L	−0.088 ± 0.007	−0.022 ± 0.010	< .001
	FEV_1, %predicted	−2.607 ± 0.239	−0.320 ± 0.342	< .001
	D_{LCO}, mL/min/mm Hg	−0.524 ± 0.045	−0.142 ± 0.065	< .001
	D_{LCO}, %predicted	−2.199 ± 0.206	−0.482 ± 0.297	< .001
	Cyst score, %	0.930 ± 0.150	−0.142 ± 0.221	< .001
Histogram	**Mean**	**2.626 ± 0.862**	**−2.765 ± 1.275**	**< .001**
	Skewness	0.011 ± 0.004	−0.002 ± 0.006	.060
	Kurtosis	**0.036 ± 0.009**	**−0.003 ± 0.013**	**.009**
Co-occurrence matrix	**Energy**	**1.105 ± 0.187**	**−0.091 ± 0.274**	**< .001**
	Inverse difference	**0.008 ± 0.002**	**−0.002 ± 0.003**	**.002**
	Entropy	**0.050 ± 0.010**	**−0.008 ± 0.015**	**.002**
	Sum entropy	**2.773 ± 0.595**	**−0.406 ± 0.873**	**.002**
	Difference entropy	**2.035 ± 0.479**	**−0.467 ± 0.706**	**.003**
	Sum average	3.224 ± 1.650	−1.898 ± 2.533	.089
	Difference average	0.397 ± 0.100	0.120 ± 0.149	.113
Run length	**Short run emphasis**	**0.006 ± 0.002**	**−0.002 ± 0.002**	**< .001**
	Long run emphasis	**0.315 ± 0.053**	**−0.045 ± 0.077**	**< .001**
	Gray-level nonuniformity	0.138 ± 0.055	−0.022 ± 0.082	.095
	Run-length nonuniformity	**0.860 ± 0.212**	**−0.186 ± 0.312**	**.005**
	Run percentage	**0.021 ± 0.004**	**−0.004 ± 0.006**	**< .001**
	Low-gray run emphasis	**0.009 ± 0.002**	**−0.001 ± 0.003**	**.004**
	Short run low-gray emphasis	−0.0004 ± 0.0003	−0.001 ± 0.0005	.349
	Long run low-gray emphasis	**0.379 ± 0.060**	**−0.042 ± 0.088**	**< .001**

All analyses were adjusted for the initial values of each outcome variable. Texture properties were calculated as the absolute difference in texture between regions near cysts and away from cysts. Texture properties in bold showed statistically significant ($P < .05$) changes in rate during sirolimus treatment. e-Table 1 provides descriptive statistics of the parameters and *P* values to five decimal places. D_{LCO} = diffusion capacity for carbon monoxide; PFT = pulmonary function test.

is essential to reflect lung changes. These texture properties have also been used in biomedical imaging to characterize or classify tissue/bone.[33-38]

Limitations

HRCT imaging might be affected by patient breathing or movement during the scan. We limited this effect by using a large sample of pixels within a single scan. The CT scans used in this investigation were collected over a 10-year period, and variability in imaging protocol and use of older CT scanners might have contributed to some differences. We reduced these effects by calculating texture differences between regions near and away from cysts on the same CT scan. Texture calculations in regions away from cysts served as independent, individualized controls for each CT scan, which eliminated some variability between studies.

Because this is an exploratory study, the multitude of statistical tests have not been adjusted for multiple testing, and therefore, some findings deemed significant may be due to chance. We have provided P values to five decimal places (e-Tables 1-4) to allow for ad hoc adjustment. The conclusions of the study may only be applicable to a population of patients with LAM and clinical phenotypes similar to that of the patients of the longitudinal study. Because the longitudinal study examined the effect of sirolimus treatment on the association of the texture properties with pulmonary function, the patients of the longitudinal study may be sicker than the general LAM population.

Conclusions

Texture analysis of HRCTs can serve as a tool to measure lung texture degradation in LAM. We have

TABLE 5] Associations of Texture Properties With FEV_1, DLCO, and Cyst Score in Patient Visits Before Sirolimus Treatment, as Well as in All Patient Visits (Including Visits When Receiving Sirolimus Treatment), Using Mixed Effects Models

		FEV_1		DLCO		Cyst Score	
	Parameter	Pretreatment Visits Only	All Visits[a]	Pretreatment Visits Only	All Visits[a]	Pretreatment Visits Only	All Visits[a]
	Cyst score	< .001	< .001	< .001	< .001		
Histogram	Mean	.006	< .001	.066	.041	< .001	< .001
	Skewness	.309	< .001	.720	.453	.002	< .001
	Kurtosis	.411	.120	.918	.598	.011	< .001
Co-occurrence matrix	**Energy**	**< .001**	**< .001**	**.003**	**.001**	**< .001**	**< .001**
	Inverse difference	**.001**	**< .001**	**.006**	**< .001**	**< .001**	**< .001**
	Entropy	**< .001**	**< .001**	**.004**	**< .001**	**< .001**	**< .001**
	Sum entropy	**.001**	**< .001**	**.008**	**.001**	**< .001**	**< .001**
	Difference entropy	**.003**	**< .001**	**.017**	**.001**	**< .001**	**< .001**
	Sum average	.070	< .001	.202	.013	.227	.795
	Difference average	.059	< .001	.003	.008	< .001	< .001
Run length	**Short run emphasis**	**.001**	**< .001**	**.005**	**.001**	**< .001**	**< .001**
	Long run emphasis	**.001**	**< .001**	**.004**	**.003**	**< .001**	**< .001**
	Gray-level nonuniformity	.064	< .001	.125	.039	< .001	<.001
	Run-length nonuniformity	**< .001**	**< .001**	**.005**	**.002**	**< .001**	**< .001**
	Run percentage	**< .001**	**< .001**	**.002**	**< .001**	**< .001**	**< .001**
	Low-gray run emphasis	**< .001**	**< .001**	**< .001**	**< .001**	**< .001**	**< .001**
	Short run low-gray emphasis	.010	< .001	.259	.124	.002	.006
	Long run low-gray emphasis	**< .001**	**< .001**	**< .001**	**< .001**	**< .001**	**< .001**

All associations are adjusted for initial values of respective parameters. Texture properties in bold show significant correlation to FEV_1, DLCO, and cyst score for both pretreatment and all visits. e-Tables 2-4 provide descriptive statistics of the parameters and *P* values to five decimal places. See Table 4 legend for expansion of abbreviation.

[a]The effect of various textures on the outcome variables (FEV_1, DLCO, cyst score) was independent of sirolimus treatment, which was a significant predictor of these outcome variables. The statistical interaction of texture and sirolimus treatment was used to assess whether the effect of a texture property on an outcome was different in the context of no treatment or sirolimus treatment. Because the statistical interaction of each texture variable and treatment with sirolimus was not significant, we combined all visits (and adjusted for sirolimus treatment) to assess the relationship of textures and each of the outcome variables.

identified 11 texture properties that track lung changes that were validated in cross-sectional and longitudinal studies, as well as with correlations with pulmonary function data. As cyst score increases, lung texture degradation occurs in areas surrounding cysts. Sirolimus improves lung texture in areas surrounding cysts and reduces cyst scores. We also found that the texture measures that incorporate spatial information into calculations are better at detecting tissue changes. Cyst scores may be a better biomarker to follow disease progression and treatment than pulmonary function tests, because a healthy person with no lung disease may have FEV_1 and DLCO of 80% to 120% of predicted as a normal baseline, but the cyst score would be < 1%. Abnormalities and changes in cyst score may be detected before pulmonary function decreases below the normal range.

As image quality and resolution continue to advance in medical imaging, texture analysis will become more sensitive to tissue changes. The use of CT in women of childbearing age is a concern because of the risks of radiation exposure. The texture determinations

presented here were calculated using preexisting CT scans and did not require additional radiation exposure. We have developed procedures to lower the radiation dose necessary to quantify cyst score to minimize patient risk[39] and are testing them on texture properties. The findings presented here are broadly relevant to any disease involving general lung tissue damage. Texture analysis of HRCT imaging can supplement clinical findings to provide greater understanding of disease status and progression.

Acknowledgments

Author contributions: J. M. takes responsibility for the content of the manuscript, including the data and analysis. Study concept and design: V. G., J. Y., and J. M. Acquisition, analysis, or interpretation of data: all authors. Drafting of the manuscript: V. G., W. K. S., and J. M. Critical revision of the manuscript for important intellectual design: all authors. Statistical analysis: V. G. and M. S. Administrative, technical, or material support: N. A. A., A.M.T ., and M. Y. C. Study supervision: J. Y. and J. M. Providing final approval of the version to be published: all authors. Agreeing to be accountable for all aspects of the work in ensuring that questions related to the accuracy or integrity of any part of the work are appropriately investigated and resolved: all authors.

Financial/nonfinancial disclosures: None declared.

Role of sponsors: The sponsor had no role in the design of the study, the collection and analysis of the data, or the preparation of the manuscript.

Additional information: The e-Appendix and e-Tables can be found in the Supplemental Materials section of the online article.

References

1. McCormack FX, Gupta N, Finlay GR, et al. Official American Thoracic Society/ Japanese Respiratory Society Clinical Practice Guidelines: Lymphangioleiomyomatosis Diagnosis and Management. *Am J Respir Crit Care Med*. 2016;194(6):748-761.
2. Johnson SR, Taveira-DaSilva AM, Moss J. *Lymphangioleiomyomatosis.* Clin Chest Med. 2016;37(3):389-403.
3. Henske EP, McCormack FX. Lymphangioleiomyomatosis - a wolf in sheep's clothing. *J Clin Invest*. 2012;122(11):3807-3816.
4. Johnson SR, Cordier JF, Lazor R, et al. European Respiratory Society guidelines for the diagnosis and management of lymphangioleiomyomatosis. *Eur Respir J*. 2010;35(1):14-26.
5. Muzykewicz DA, Sharma A, Muse V, Numis AL, Rajagopal J, Thiele EA. TSC1 and TSC2 mutations in patients with lymphangioleiomyomatosis and tuberous sclerosis complex. *J Med Genet*. 2009;46(7):465-468.
6. Crino PNK, Petri E. The tuberous sclerosis complex. *N Engl J Med*. 2007;356(1):92-94.
7. Carsillo T, Astrinidis A, Henske EP. Mutations in the tuberous sclerosis complex gene TSC2 are a cause of sporadic pulmonary lymphangioleiomyomatosis. *Proc Natl Acad Sci U S A*. 2000;97(11):6085-6090.
8. Sengupta S, Peterson TR, Sabatini DM. Regulation of the mTOR complex 1 pathway by nutrients, growth factors, and stress. *Molec Cell*. 2010;40(2):310-322.
9. McCormack FX, Inoue Y, Moss J, et al. Efficacy and safety of sirolimus in lymphangioleiomyomatosis. *N Engl J Med*. 2011;364(17):1595-1606.
10. Yao J, Taveira-DaSilva AM, Jones AM, Julien-Williams P, Stylianou M, Moss J. Sustained effects of sirolimus on lung function and cystic lung lesions in lymphangioleiomyomatosis. *Am J Respir Crit Care Med*. 2014;190(11):1273-1282.
11. Dabora SL, Franz DN, Ashwal S, et al. Multicenter phase 2 trial of sirolimus for tuberous sclerosis: kidney angiomyolipomas and other tumors regress and VEGF- D levels decrease. *PloS One*. 2011;6(9):e23379.
12. Bissler JJ, McCormack FX, Young LR, et al. Sirolimus for angiomyolipoma in tuberous sclerosis complex or lymphangioleiomyomatosis. *N Engl J Med*. 2008;358(2):140-151.
13. Taveira-DaSilva AM, Hathaway O, Stylianou M, Moss J. Changes in lung function and chylous effusions in patients with lymphangioleiomyomatosis treated with sirolimus. *Ann Intern Med*. 2011;154(12):797-805.
14. Ohno Y, Takenaka D, Kanda T, et al. Adaptive iterative dose reduction using 3D processing for reduced- and low-dose pulmonary CT: comparison with standard-dose CT for image noise reduction and radiological findings. *AJR Am J Roentgenol*. 2012;199(4):W477-W485.
15. Prasad SR, Wittram C, Shepard JA, McLoud T, Rhea J. Standard-dose and 50%-reduced-dose chest CT: comparing the effect on image quality. *AJR. Am J Roentgenol*. 2002;179(2):461-465.
16. National Lung Screening Trial Research Team, Adams AM, Berg CD, Black WC, et al. Reduced lung-cancer mortality with low-dose computed tomographic screening. *N Engl J Med*. 2011;365(5):395-409.
17. Jaklitsch MT, Jacobson FL, Austin JH, et al. The American Association for Thoracic Surgery guidelines for lung cancer screening using low-dose computed tomography scans for lung cancer survivors and other high-risk groups. *J Thorac Cardiovasc Surg*. 2012;144(1):33-38.
18. Avila NA, Kelly JA, Dwyer AJ, Johnson DL, Jones EC, Moss J. Lymphangioleiomyomatosis: correlation of qualitative and quantitative thin-section CT with pulmonary function tests and assessment of dependence on pleurodesis. *Radiology*. 2002;223(1):189-197.
19. Paciocco G, Uslenghi E, Bianchi A, et al. Diffuse cystic lung diseases: correlation between radiologic and functional status. *Chest*. 2004;125(1):135-142.
20. Yao J, Taveira-DaSilva AM, Colby TV, Moss J. CT grading of lung disease in lymphangioleiomyomatosis. *AJR Am J Roentgenol*. 2012;199(4):787-793.
21. Argula RG, Kokosi M, Lo P, et al. A novel quantitative computed tomographic analysis suggests how sirolimus stabilizes progressive air trapping in lymphangioleiomyomatosis. *Ann Am Thorac Soc*. 2016;13(3):342-349.
22. Haidekker MA. *Advanced Biomedical Image Analysis*. Hoboken, NJ: John Wiley & Sons; 2011.
23. Bankman IN. *Handbook of Medical Imaging: Processing and Analysis*. San Diego, CA: Academic Press; 2000.
24. Haralick RM, Shanmugam K. Textural features for image classification. *IEEE Trans Syst Man Cybernetics*. 1973;3(6): 610-621.
25. Sluimer I, Schilham A, Prokop M, van Ginneken B. Computer analysis of computed tomography scans of the lung: a survey. *IEEE Trans Med Imaging*. 2006;25(4):385-405.
26. Van Rikxoort EM dHB, van de Vorst S, Prokop M, van Ginneken B. Automatic segmentation of pulmonary segments from volumetric chest CT scans. *IEEE Trans Med Imaging*. 2009;28(4):621-630.
27. Uppaluri R, Hoffman EA, Sonka M, Hartley PG, Hunninghake GW, McLennan G. Computer recognition of regional lung disease patterns. *Am J Respir Crit Care Med*. 1999;160(2):648-654.
28. Miller MR, Hankinson J, Brusasco V, et al. Standardisation of spirometry. *Eur Respir J*. 2005;26(2):319-338.
29. Macintyre N, Crapo RO, Viegi G, et al. Standardisation of the single-breath determination of carbon monoxide uptake in the lung. *Eur Respir J*. 2005;26(4):720-735.
30. van der Bruggen-Bogaarts BA, Broerse JJ, Lammers JW, van Waes PF, Geleijns J. Radiation exposure in standard and

high-resolution chest CT scans. *Chest*. 1995;107(1):113-115.

31. Matsui K, Takeda K, Yu ZX, Travis WD, Moss J, Ferrans VJ. Role for activation of matrix metalloproteinases in the pathogenesis of pulmonary lymphangioleiomyomatosis. *Arch Pathol Lab Med*. 2000;124(2):267-275.
32. Xu X, Dai H, Geng J, et al. Rapamycin increases CCN2 expression of lung fibroblasts via phosphoinositide 3-kinase. *Lab Investig*. 2015;95(8):846-859.
33. Mahmoud-Ghoneim D, Cherel Y, Lemaire L, de Certaines JD, Maniere A. Texture analysis of magnetic resonance images of rat muscles during atrophy and regeneration. *Magn Reson Imaging*. 2006;24(2):167-171.
34. Shamir L, Wolkow CA, Goldberg IG. Quantitative measurement of aging using image texture entropy. *Bioinformatics*. 2009;25(23):3060-3063.
35. Chen W, Giger ML, Li H, Bick U, Newstead GM. Volumetric texture analysis of breast lesions on contrast-enhanced magnetic resonance images. *Magn Reson Med*. 2007;58(3):562-571.
36. Virmani JKV, Kalra N, Khandelwal N. Prediction of liver cirrhosis based on multiresolution texture descriptors from B-mode ultrasound. *Int J Convergence Comp*. 2013;1(1):19-37.
37. Ardakani AAMA, Gharbali A, Rostami A. Diagnosis of breast tumors with sonographic texture analysis using run-length matrix. *Int J Cancer Manage*. 2018;11(2):e6120.
38. Ito M, Ohki M, Hayashi K, Yamada M, Uetani M, Nakamura T. Trabecular texture analysis of CT images in the relationship with spinal fracture. *Radiology*. 1995;194(1):55-59.
39. Hu-Wang E, Schuzer JL, Rollison S, et al. Chest CT scan at radiation dose of a posteroanterior and lateral chest radiograph series: a proof of principle in lymphangioleiomyomatosis. *Chest*. 2019;155(3):528-533.